BJR

https://doi.org/10.1259/bjr.20190221

Received: 27 February 2019 | Revised: 22 July 2019 | Accepted: 02 October 2019

Cite this article as:
Lockard CA, Chang A, Clanton TO, Ho CP. T2* mapping and subregion analysis of the tibialis posterior tendon using 3 Tesla magnetic resonance imaging. *Br J Radiol* 2019; **92**: 20190221.

FULL PAPER

T2* mapping and subregion analysis of the tibialis posterior tendon using 3 Tesla magnetic resonance imaging

[1]CARLY ANNE LOCKARD, M.S., [1]ANGELA CHANG, M.D., [2]THOMAS O CLANTON, M.D. and [1]CHARLES P HO, M.D., Ph.D.

[1]Steadman Philippon Research Institute, 181 West Meadow Drive, Suite 1000 Vail, Colorado 81657, United States
[2]The Steadman Clinic, 181 West Meadow Drive, Suite 400 Vail, Colorado 81657, United States

Address correspondence to: Dr Charles P Ho
E-mail: *charles.ho@sprivail.org*

Objective: Early detection of tibialis posterior tendon changes and appropriate intervention is necessary to prevent disease progression to flat-foot deformity and foot/ankle dysfunction, and the need for operative treatment. Currently, differentiating between early-stage tibialis posterior tendon deficiency patients who will benefit from conservative *vs* more aggressive treatment is challenging. The objective of this work was to establish a quantitative MRI T2* mapping method and subregion baseline values in the tibialis posterior tendon in asymptomatic ankles for future clinical application in detecting tendon degeneration.

Methods: 26 asymptomatic volunteers underwent T2* mapping. The tendon was divided axially into seven subregions. Summary statistics for T2* within each subregion were calculated and compared using Tukey post-hoc pairwise comparisons.

Results: Results are reported for 24 subjects. The mean tibialis posterior tendon T2* was 7 ± 1 ms. Subregion values ranged from 6 ± 1 to 9 ± 2 ms with significant between-region differences in T2*. Inter- and intrarater absolute agreement intraclass correlation coefficient (ICC) values were all "excellent" (0.75 < ICC=1.00) except for regions 5 through 7, which had "fair to good" interrater and/or and intrarater ICC values (0.4 < ICC=0.75).

Conclusion: A tibialis posterior tendon T2* mapping protocol, subregion division method, and baseline T2* values for clinically relevant regions were established. Significant differences in T2* were observed along the tendon length.

Advances in knowledge: This work demonstrates that regional variation exists and should be considered for future T2*-based research on posterior tibias tendon degeneration and when using T2* mapping to evaluate for potential tibialis posterior tendon degeneration.

INTRODUCTION

Tibialis posterior tendon (TPT) deficiency can lead to flat-foot deformity and functional dysfunction in even low-intensity daily activities such as walking.[1–3] The TPT can be injured during athletic activity,[4–6] but more commonly undergoes progressive degenerative changes without a specific initiating event,[7] making the etiology unclear. There is an elevated risk of TPT deficiency in older women[8] and individuals with obesity,[9] diabetes,[10] concomitant ligamentous foot and ankle pathologies, and/or inflammatory diseases such as rheumatoid arthritis.[11] Early detection and appropriate intervention may prevent development of severe degeneration of the TPT and overload of other medial arch supporting structures[7] and the need for operative treatment.[12]

Conventional MRI TPT dysfunction grading scores are correlated to functional deficiencies, but not to degenerative histological changes[13] such as decreased collagen organization and decreased Type I collagen, hyalinization, increased proteoglycan content, and neovascularization.[13–15] Quantitative MRI may be more sensitive to these early microstructural changes that occur prior to the compromise of function.

Quantitative T2 and T2-star (T2*) MRI mapping allow objective, non-invasive assessment of water content and collagen organization, with T2* being especially applicable in highly organized tissues such as tendon.[16,17] T2* and T2 mapping values have been correlated to factors associated with tendinopathy in the Achilles[16,18–20] and patellar[21] tendons, including increased collagen disorganization and free water content, as well as healing changes after treatment in a rabbit Achilles model.[22] T2 mapping values have also been shown to be significantly increased with tendinosis and tears of the supraspinatus tendon.[23] However, these

techniques have not yet been applied to the TPT *in vivo* in human subjects.

Development of TPT-specific methodology for positioning and subregion analysis is needed to optimize for patient studies. Prior T2 and T2* mapping work in Achilles, peroneal, and rotator cuff tendons shows that tendon quantitative mapping values vary spatially within tendons even in asymptomatic subjects[20,24,25] and that this spatial variation is tendon-specific. TPT-specific subregions and baseline values need to be established to account for tendon specific spatial variation. TPT subregion-specific baseline values are needed due to tendon curvature and the resulting magic angle effects[26] and variation in histology along the length of the tendon,[10,27] both of which may influence T2* values. The use of clinically relevant tendon subregions is also important for focused analysis of high-risk regions, such as the avascular, fibrocartilage-like retromalleolar zone,[27] which is the most common site of degenerative tearing.[10,11] The objective of this work was to establish a quantitative MRI T2* mapping method and tendon-specific subregion baseline values in the tibialis posterior tendon in asymptomatic ankles for future clinical application in detecting tendon degeneration.

METHODS AND MATERIALS

This prospective cohort study was approved by the Vail Health Hospital Institutional Review Board and all subjects provided informed consent. 26 subjects aged 18–62 years were recruited between January and April 2014 at The Steadman Clinic, Vail, CO, USA and screened using a self-evaluation questionnaire for ankle/hindfoot symptoms and injury history, as well as a standard clinical examination by an orthopaedic foot and ankle surgeon. Exclusion criteria included previous ankle surgery or injury, history of systemic inflammatory or crystalline joint disease, osteoarthritis, calcific tendonitis, or tendon damage found on the subsequent MRI. 2 subjects were excluded for abnormalities seen on the morphological MR images resulting in a final subject group of 11 female and 13 male subjects (9 males/0 females in the 18–32 years age group, 3 males/5 females in the 33–47 group, and 1 male/6 females in the 48–62 group; overall age range 23–62 years).

Unilateral ankle/hindfoot MRI was performed with a Siemens Magnetom Verio 3 T scanner (Siemens Medical Solutions, Erlangen, Germany) with a gradient strength of 40 mT/m. Volunteers were positioned prone with the imaged ankle in passive plantarflexion stabilized with foam inserts in the centre of an 8-channel receive knee coil (Invivo, Gainesville, FL). The prone position was used to straighten the tendons parallel to the main magnetic field to reduce the magic angle effect. 12 left and 12 right ankles were scanned.

The scanning protocol included a clinical sequence and an axial-plane multiecho gradient-echo T2* mapping sequence performed approximately 8 min after participants entered the scanner. Table 1 lists the parameters for the T2* mapping sequence. T2* values were calculated using a pixelwise, monoexponential, non-negative least square fit to the decay curve including all mapping echoes (Siemens MapIt, Siemens Medical Solutions, Erlangen, Germany).

Table 1. Magnetic resonance imaging acquisition parameters for T2* mapping sequence

Plane	Axial
Repetition time (milliseconds)	1121
Echo time (milliseconds)	3.25,9.00,15.33,21.66,28.00
Field of view (milliseconds)	140
Matrix	256 × 256
Voxel size (millimeters)	0.55 × 0.55 × 2.50
Slice thickness (millimeters)	2.50
Slice spacing (millimeters)	3.00
Number of slices	34
Examination time (minutes:seconds)	4:47

The TPT was manually segmented using a stylus and touchscreen (WACOM Cintiq, Wacom Technology Corporation, Portland, OR) in Mimics (Materialise, Plymouth, MI) on each slice of the T2* mapping sequence third echo (echo time = 15.33 ms) by two raters, a research engineer [Rater 1] and a third-year medical student [Rater 2] with approximately 2 and 1 year(s) of experience with musculoskeletal MRI segmentation, respectively. The segmentation accuracy was reviewed by a senior musculoskeletal radiologist with 28 years of experience (C.P.H.). The raters were instructed to stop segmentation where the tendon became difficult to visualize near the insertions.

Rater two performed a second segmentation round of all subjects to assess intrarater reliability. Repeat segmentation was performed following 4 weeks between rounds to avoid bias from prior rounds. Rater 1 identified the bony landmarks of the most distal point of the medial malleolus, most proximal slice in which the navicular bone was visible, and most distal slice in which the navicular bone was visible and recorded the appropriate landmark slice locations for each subject.

The segmentations were exported from Mimics as binary images and imported into a custom MATLAB program (MATLAB Release 2013a, The MathWorks, Inc., Natick, MA) along with corresponding T2* maps. The TPT segmentations were automatically overlaid on the T2* map images, defining the region of interest pixels on the corresponding T2* map images.

Seven TPT subregions along the length of the tendon were defined automatically in MATLAB using the recorded landmark slice locations. The regions were defined as follows:

Region 1: most proximal slice to third slice proximal to medial malleolus (variable length, mean 26 mm, range 6–45 mm);

Region 2: medial malleolus landmark slice and the two slices proximal (9 mm long);

Region 3: one slice distal to medial malleolus landmark slice plus next two distal slices (9 mm long);

Figure 1. Medial view of 3D volume rendering of tibialis posterior tendon overlaid on associated bones with labeled bony landmarks and tendon subregions 1 through 7. 3D, three-dimensional.

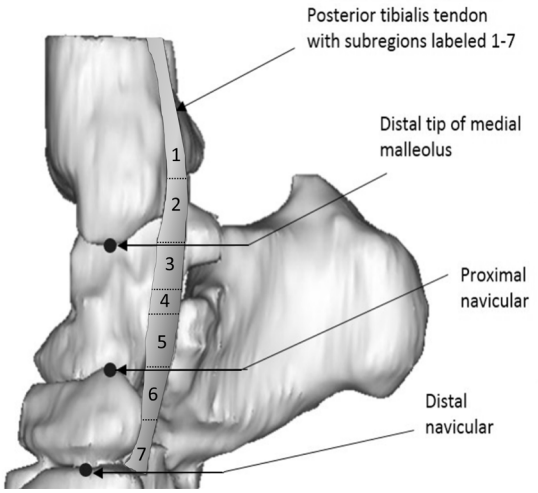

Region 4: region between regions 3 and 5 (variable length, mean 12 mm, range 3–21 mm)

Region 5: proximal navicular landmark slice and two proximal slices (9 mm long)

Region 6: one slice distal to proximal navicular landmark slice and two distal slices (9 mm long)

Region 7: fourth slice distal to proximal navicular landmark to distal navicular landmark slice (variable length, mean 9 mm, range 6–12 mm)

The TPT subregions are shown in Figure 1.

The subject median T2* values for the entire TPT and each subregion were calculated. The means and standard deviations of these median T2* values were calculated for all subjects. Statistical analyses were performed using a statistical programming language (R v. 3.2.3, R Development Core Team, Vienna, Austria). A repeated measures analysis was conducted via random-intercepts mixed-effects models (nlme: Linear and Nonlinear Mixed Effects Models, R Development Core Team). Exponential spatial correlation structure was assumed, while equal variance not assumed. Tukey post-hoc pairwise comparisons were performed to determine whether differences in mean T2* between subregions were significant ($p < 0.05$).

A two-way random effects model was used to calculate the single measures, absolute agreement version of the intraclass correlation coefficient (ICC) representing the intra- and inter-rater measurement reliability of median T2* values within each subregion and for the entire TPT. The ICC values were interpreted as follows: ICC <0.40 = poor agreement; 0.40 ≤ ICC ≤ 0.75 = fair to good agreement; ICC >0.75 = excellent agreement.[28]

RESULTS

The mean TPT T2* was 7 ± 1 (mean ± between-subject standard deviation) ms. The mean T2* values ranged from 6 ± 1 ms for the lowest mean values (region 5) to 9 ± 2 ms for the highest means values (regions 3 and 7). The inter- and intrarater absolute agreement ICC values were all in the "excellent" range (0.75 < ICC = 1.00) except for the most distal two subregions, which had inter- and intrarater ICC values in the "fair to good" range (0.4 < ICC = 0.75). The specific T2* values for each TPT subregion, as well as the inter- and intrarater absolute agreement ICC values are listed in Table 2 for Rater 1 and Rater 2.

Figure 2 shows the individual subject T2* value datapoints and the subregion medians, quartiles, and ranges over all subjects for the seven TPT subregions. Significant differences between subregions are indicated with square brackets, with asterisks indicating the specific *p*-value ranges (with *** indicating $0 < p < 0.001$, ** indicating $0.001 < p < 0.01$, and * indicating $0.01 < p < 0.05$) listed out in Table 3.

DISCUSSION

This study establishes TPT T2* mapping methodology and baseline values in asymptomatic volunteers, which can be applied

Table 2. Mean T2 ± standard deviation for each region (averaged over all raters/rounds) and subregion and inter- and intrarater absolute agreement intraclass coefficient values

Region	Mean of subject medians ± SD (milliseconds)	Inter-rater ICC (95% lower–upper bound)	Intra-rater ICC (95% lower–upper bound)
Whole tendon	7 ± 1	0.68 (0.49–0.80)	0.74 (0.58–0.86)
1	7 ± 1	0.79 (0.53–0.91)	1.0 (1.0–1.0)
2	8 ± 1	0.87 (0.69–0.95)	0.99 (0.94–1.0)
3	9 ± 2	0.78 (0.56–0.90)	0.89 (0.77–0.95)
4	7 ± 1	0.79 (0.56–0.92)	0.96 (0.88–0.99)
5	6 ± 1	0.58 (0.27–0.79)	0.88 (0.75–0.96)
6	7 ± 1	0.75 (0.51–0.87)	0.54 (0.16–0.78)
7	9 ± 2	0.66 (0.37–0.81)	0.69 (0.47–0.82)

ICC, intraclass correlation coefficient; SD, standard deviation.

Figure 2. Boxplots for TPT subregion T2* values, with plotted points indicating the median T2* value for each individual subject and the horizontal lines in each box representing the median T2* value for all subjects. The upper and lower boundaries of the box show the upper and lower quartiles. The whiskers show the highest and lowest value excluding the outliers. Significant differences in mean T2* between regions are indicated with brackets and asterisks. TPT, tibialis posterior tendon.

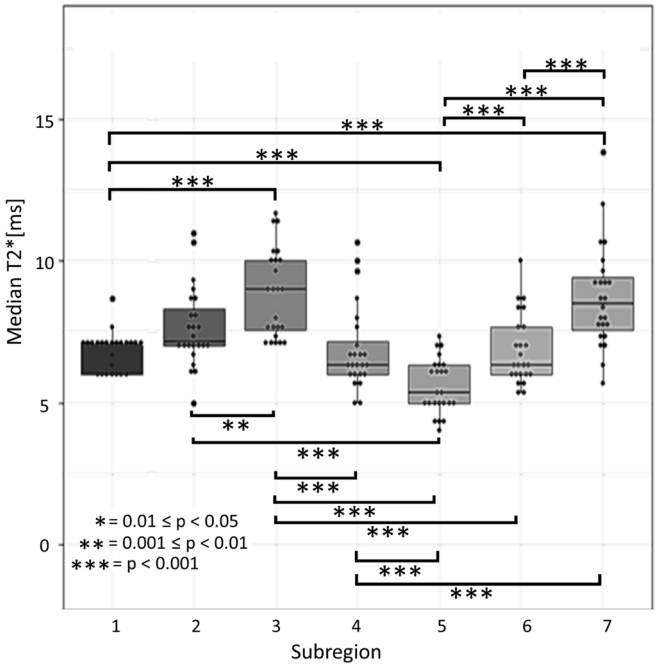

to future evaluation of patients with early TPT dysfunction and for evaluation of post-treatment tendon response. The results of this study demonstrate that there are significant differences in baseline mean T2* mapping values among anatomically relevant subregions of the TPT. These subregion differences may be explained by histological variation along the length of the tendon, such as variation in the TPT tissue fibrocartilage content due to varying stress loads placed upon the different anatomical regions. Fibrocartilage content in tendons is frequently increased in areas of compression, as well as at the tendon entheses[29] and has been shown to have slightly higher T2* values than tendon tissue.[26] The TPT has been reported to have elevated fibrocartilage content as it courses around the fulcrum of the medial malleolus and as it passes the plantar calcaneonavicular ligament.[30] These anatomical regions correspond approximately to regions 2 and 3 (medial malleolus) and regions 6 and 7 (plantar calcaneonavicular ligament) as defined in this current study. This provides possible explanation for the slightly elevated T2* in these regions, although histological correlation is needed for more definitive explanation.

Prior work in the Achilles tendon has demonstrated regional variation in T2 and T2* in the anteroposterior direction and mediolateral directions,[20] in addition to the longitudinal direction.[19] Similarly, subregion analysis has been performed for the supraspinatus tendon of the rotator cuff for anterior and posterior portions of the medial, middle, and lateral regions of the tendon/musculotendinous junction.[23] Use of such additional subdivisions parallel to the longitudinal axis of the tendon may allow detection of relatively small, localized alterations in the tendon T2* values. For example, in the rotator cuff, significant differences were found between the lateral subregion T2 values of asymptomatic *vs* tendinosis subjects when the anterior portion was compared, while no significant differences were found between these two groups for the posterior portion of the lateral subregion.[23] Similarly, in the Achilles tendon subregion differences were detected between the medial and lateral musculotendinous junction and mid-tendon subregions, as well as between the anterior and posterior mid-tendon and insertional subregions in healthy volunteers.[20] We chose to focus on T2* value variation only in the longitudinal direction in the TPT due to the small diameter of this tendon, which limits the feasibility of creating additional subregion divisions in the anteroposterior and mediolateral directions.

Currently, there is a scarcity of *in vivo* TPT quantitative mapping data in the literature for direct comparison to the values obtained in this study. However, the T2* values measured in this study are similar to those seen in other asymptomatic-volunteer ankle tendons measured with single-component methods, including the peroneal tendons (subregion mean T2* reported to range from 7 ± 2 to 14 ± 5 ms)[24] and the Achilles tendon (mean T2* reported to be approximately 3 ms)[19].

Table 3. Mean T2*± standard deviation for each region and results for significant differences between regions

Region	**Mean of subject medians ± standard deviation (milliseconds)**	***p*-value range: *** indicates $0 < p < 0.001$, ** indicates $0.001 < p < 0.01$, * indicates $0.01 < p < 0.05$**
1	7 ± 1	Region one significantly different from regions 2(**),3,5,7 (***)
2	8 ± 1	Region two significantly different from regions 1(**),3(**),5(***)
3	9 ± 2	Region three significantly different from regions 1(***),2(**),4,5,6(***)
4	7 ± 1	Region four significantly different from regions 3,5,7(***)
5	6 ± 1	Region five significantly different from regions 1,2,3,4,6,7(***)
6	7 ± 1	Region six significantly different from regions 3,5,7(***)
7	9 ± 2	Region seven significantly different from regions 1,4,5,6(***)

This study has limitations. First, this study was limited to single-component T2* mapping using widely available clinical protocol echo times. T2* with bicomponent analysis or UTE T2* mapping may be more optimal for short T2 tissues.[19–21,31] In contrast to single-component T2* mapping, bi-component T2* mapping provides more information by measuring fast relaxing water bound to the highly organized collagen fibers (T2*=0.3–1.3 ms) and slow relaxing bulk water (T2*=8.2–20.4 ms) separately.[21] Ultrashort echo time T2* mapping may be more sensitive than T2* mapping using longer echo times, as shorter initial echo times allow for more measurements in high signal-to-noise portion of the tendon decay curve, but it is not yet widely available. Short-component and mean T2* have both been found to be significantly different between healthy volunteers and patients in the Achilles[19] and patellar[21] tendons, while long-component T2* values are more variable due to the relatively low bulk-water component in tendons.[21] We were limited by the available minimal echo time of 3.25 ms, which is in line with other currently available clinical sequences.[31]

Another limitation of this study is that some subject-specific characteristics were not controlled. Subject activity level prior to scanning was not controlled, which could lead to variation in tendon hydration levels between subjects.[32] Future tendon T2* mapping studies may benefit from inclusion of a consistent activity restriction period prior to scanning, as well as recruitment of sufficient numbers of subjects from both low and high loading activity participation levels to allow analysis of the influence of subject physical activity on baseline tendon T2* values. Subjects were not screened for contralateral ankle injury/symptoms, which could cause gait changes affecting both lower limbs. In addition, subjects were not screened for diabetes, which has been shown to have influence on tissue health and some quantitative MRI values such as high-field MRI sodium imaging values.[33] Fourth, the subject group contained an uneven distribution of male and female subjects in the youngest *vs* oldest age groups, making analysis of the influence of age and sex unfeasible. Because older females are at elevated risk of TPT deficiency,[8] future work focusing on establishing baseline values specific to this group would be beneficial. Lastly, more precise physical positioning of patient with specific plantar-flexion angle and controlled inversion/eversion could reduce potential for increased T2* due to magic angle effects[26] and provide more controlled tendon excursion for precise subregion selection.

The scan-rescan reproducibility and longitudinal study of tendon T2* mapping values remains to be assessed. Although some short-term changes in off-resonance saturation effects have been seen in the Achilles tendon following vigorous exercise,[32] indicating that excessive pre-scan loading can influence tendon properties on MRI, a scan–rescan repeatability study of patellar tendon UTE bicomponent T2* analysis for subjects who did not undergo pre-scan loading and maintained unloading between scans found only 3.8–4.8% coefficient of variation for repeat scans.[21]

The T2* values measured in this study provide important baseline results for comparison to T2* alterations in patients. T2* mapping of medial foot/ankle ligaments which are prone to overloading in the case of TPT deficiency, in addition to mapping of the TPT itself, may provide additional information about both the natural history and treatment effects for TPT deficiency and presents an interesting opportunity for future work.

In conclusion, significant differences in mean T2* were found to exist between subregions along the length of the TPT. Subregion analysis of the TPT has the potential to provide important subregion-specific information on tendon changes in patients, which is important due to the normal histological variation along the course of the tendon and the existence of specific high-risk locations along the TPT length for injury, degeneration, and rupture.

ACKNOWLEDGMENT

The authors thank Bill Brock for assistance with image acquisition and Grant Dornan for guidance during the statistical analysis.

FUNDING

This research did not receive any specific grant from funding agencies in the public, commercial, or not-for-profit sectors.

CONFLICTS OF INTEREST

Carly A. Lockard: No individual conflicts of interest to declare. Angela Chang: No individual conflicts of interest to declare. Charles P. Ho: Steadman Philippon Research Institute (Research Advisory Committee), Smith & Nephew (Consultant) Thomas O. Clanton: Arthrex, Inc. (Consultant/speaker fees, and royalties and in-kind donations of surgical supplies for research), Stryker, Inc. (Consultant/speaker fees), Small Bone Innovations (Consultant/speaker fees), Wright Medical Technology (Consultant/speaker fees), Saunders/Mosby-Elsevier (Publication royalties), Steadman Philippon Research Institute (Research Advisory Committee) Institutional disclosure: Steadman Philippon Research Institute (SPRI) exercises special care to identify any financial interests or relationships related to research conducted here. During the past calendar year, SPRI has received grant funding or in-kind donations from Arthrex, DJO, MLB, Ossur, Siemens, Smith & Nephew and XTRE.

REFERENCES

1. Mann RA, Thompson FM. Rupture of the posterior tibial tendon causing flat foot. surgical treatment. *J Bone Joint Surg Am* 1985; **67**: 556–61. doi: https://doi.org/10.2106/00004623-198567040-00009
2. Pomeroy GC, Pike RH, Beals TC, Manoli A. Acquired flatfoot in adults due to dysfunction of the posterior tibial tendon. *J Bone Joint Surg Am* 1999; **81**: 1173–82. doi: https://doi.org/10.2106/00004623-199908000-00014

3. Tome J, Nawoczenski DA, Flemister A, Houck J. Comparison of foot kinematics between subjects with posterior tibialis tendon dysfunction and healthy controls. *J Orthop Sports Phys Ther* 2006; **36**: 635–44. doi: https://doi.org/10.2519/jospt.2006.2293
4. Porter DA, Baxter DE, Clanton TO, Klootwyk TE. Posterior tibial tendon tears in young competitive athletes: two case reports. *Foot Ankle Int* 1998; **19**: 627–30. doi: https://doi.org/10.1177/107110079801900911
5. Marcus RE, Goodfellow DB, Pfister ME. The difficult diagnosis of posterior tibialis tendon rupture in sports injuries. *Orthopedics* 1995; **18**: 715–21.
6. Jacoby SM, Slauterbeck JR, Raikin SM. Acute posterior tibial tendon tear in an ice-hockey player: a case report. *Foot Ankle Int* 2008; **29**: 1045–8. doi: https://doi.org/10.3113/FAI.2008.1045
7. Arangio GA, Salathe EP. A biomechanical analysis of posterior tibial tendon dysfunction, medial displacement calcaneal osteotomy and flexor digitorum longus transfer in adult acquired flat foot. *Clin Biomech* 2009; **24**: 385–90. doi: https://doi.org/10.1016/j.clinbiomech.2009.01.009
8. Holmes GB, Mann RA. Possible epidemiological factors associated with rupture of the posterior tibial tendon. *Foot Ankle* 1992; **13**: 70–9. doi: https://doi.org/10.1177/107110079201300204
9. Van Boerum DH, Sangeorzan BJ. Biomechanics and pathophysiology of flat foot. *Foot Ankle Clin* 2003; **8**: 419–30. doi: https://doi.org/10.1016/S1083-7515(03)00084-6
10. Petersen W, Hohmann G, Stein V, Tillmann B. The blood supply of the posterior tibial tendon. *J Bone Joint Surg Br* 2002; **84-B**: 141–4. doi: https://doi.org/10.1302/0301-620X.84B1.0840141
11. Schweitzer ME, Karasick D. Mr imaging of disorders of the posterior tibialis tendon. *AJR Am J Roentgenol* 2000; **175**: 627–35. doi: https://doi.org/10.2214/ajr.175.3.1750627
12. Carmody D, Bubra P, Keighley G, Rateesh S. Posterior tibial tendon dysfunction: an overlooked cause of foot deformity. *J Fam Med Primary Care* 2015; **4**: 26. doi: https://doi.org/10.4103/2249-4863.152245
13. Albano D, Martinelli N, Bianchi A, Romeo G, Bulfamante G, Galia M, et al. Posterior tibial tendon dysfunction: clinical and magnetic resonance imaging findings having histology as reference standard. *Eur J Radiol* 2018; **99**: 55–61. doi: https://doi.org/10.1016/j.ejrad.2017.12.005
14. Gonçalves-Neto J, Witzel SS, Teodoro WR, Carvalho-Júnior AE, Fernandes TD, Yoshinari HH. Changes in collagen matrix composition in human posterior tibial tendon dysfunction. *Joint Bone Spine* 2002; **69**: 189–94. doi: https://doi.org/10.1016/S1297-319X(02)00369-X
15. Hodgson RJ, O'Connor PJ, Grainger AJ. Tendon and ligament imaging. *Br J Radiol* 2012; **85**: 1157–72. doi: https://doi.org/10.1259/bjr/34786470
16. Gärdin A, Rasinski P, Berglund J, Shalabi A, Schulte H, Brismar TB. T2 * relaxation time in Achilles tendinosis and controls and its correlation with clinical score. *J Magn Reson Imaging* 2016; **43**: 1417–22. doi: https://doi.org/10.1002/jmri.25104
17. Biercevicz AM, Murray MM, Walsh EG, Miranda DL, Machan JT, Fleming BC. T2 * Mr relaxometry and ligament volume are associated with the structural properties of the healing ACL. *J Orthop Res* 2014; **32**: 492–9. doi: https://doi.org/10.1002/jor.22563
18. Grosse U, Syha R, Hein T, Gatidis S, Grözinger G, Schabel C, et al. Diagnostic value of T1 and T2 * relaxation times and off-resonance saturation effects in the evaluation of Achilles tendinopathy by MRI at 3T. *J Magn Reson Imaging* 2015; **41**: 964–73. doi: https://doi.org/10.1002/jmri.24657
19. Juras V, Apprich S, Szomolanyi P, Bieri O, Deligianni X, Trattnig S. Bi-exponential T2 analysis of healthy and diseased Achilles tendons: an in vivo preliminary magnetic resonance study and correlation with clinical score. *Eur Radiol* 2013; **23**: 2814–22. doi: https://doi.org/10.1007/s00330-013-2897-8
20. Juras V, Zbyn S, Pressl C, Valkovic L, Szomolanyi P, Frollo I, et al. Regional variations of T_2* in healthy and pathologic Achilles tendon in vivo at 7 Tesla: preliminary results. *Magn Reson Med* 2012; **68**: 1607–13. doi: https://doi.org/10.1002/mrm.24136
21. Kijowski R, Wilson JJ, Liu F. Bicomponent ultrashort echo time T2* analysis for assessment of patients with Patellar tendinopathy: ultrashort te T2* analysis of tendinopathy. *J Magn Reson Imaging* 2017; **46**: 1441–7.
22. Fukawa T, Yamaguchi S, Watanabe A, Sasho T, Akagi R, Muramatsu Y, et al. Quantitative assessment of tendon healing by using Mr T2 mapping in a rabbit Achilles tendon transection model treated with platelet-rich plasma. *Radiology* 2015; **276**: 748–55. doi: https://doi.org/10.1148/radiol.2015141544
23. Ganal E, Ho CP, Wilson KJ, Surowiec RK, Smith WS, Dornan GJ, et al. Quantitative MRI characterization of arthroscopically verified supraspinatus pathology: comparison of tendon tears, tendinosis and asymptomatic supraspinatus tendons with T2 mapping. *Knee Surg Sports Traumatol Arthrosc* 2016; **24**: 2216–24. doi: https://doi.org/10.1007/s00167-015-3547-2
24. Wilson KJ, Surowiec RK, Johnson NS, Lockard CA, Clanton TO, Ho CP. T2* mapping of peroneal tendons using clinically relevant subregions in an asymptomatic population. *Foot Ankle Int* 2017; **38**: 677–83. doi: https://doi.org/10.1177/1071100717693208
25. Anz AW, Lucas EP, Fitzcharles EK, Surowiec RK, Millett PJ, Ho CP. Mri T2 mapping of the asymptomatic supraspinatus tendon by age and imaging plane using clinically relevant subregions. *Eur J Radiol* 2014; **83**: 801–5. doi: https://doi.org/10.1016/j.ejrad.2014.02.002
26. Du J, Pak BC, Znamirowski R, Statum S, Takahashi A, Chung CB, et al. Magic angle effect in magnetic resonance imaging of the Achilles tendon and enthesis. *Magn Reson Imaging* 2009; **27**: 557–64. doi: https://doi.org/10.1016/j.mri.2008.09.003
27. Vogel KG, Ördög A, Pogány G, Oláh J. Proteoglycans in the compressed region of human tibialis posterior tendon and in ligaments. *Journal of Orthopaedic Research* 1993; **11**: 68–77. doi: https://doi.org/10.1002/jor.1100110109
28. Fleiss JL. *The design and analysis of clinical experiments*. New York, NY: John Wiley & Sons, Inc.;; 19867 p..
29. Benjamin M, Ralphs JR. Fibrocartilage in tendons and ligaments--an adaptation to compressive load. *J Anat* 1998; **193 (Pt 4**: 481–94. doi: https://doi.org/10.1046/j.1469-7580.1998.19340481.x
30. Benjamin M, Qin S, Ralphs JR. Fibrocartilage associated with human tendons and their pulleys. *J Anat* 1995; **187 (Pt 3**: 625–33.
31. Siriwanarangsun P, Bae WC, Statum S, Chung CB. Advanced MRI techniques for the ankle. *AJR Am J Roentgenol* 2017; **209**: 511–24. doi: https://doi.org/10.2214/AJR.17.18057
32. Syha R, Springer F, Grözinger G, Würslin C, Ipach I, Ketelsen D, et al. Short-Term exercise-induced changes in hydration state of healthy Achilles tendons can be visualized by effects of off-resonant radiofrequency saturation in a three-dimensional ultrashort echo time MRI sequence applied at 3 tesla. *J Magn Reson Imaging* 2014; **40**: 1400–7. doi: https://doi.org/10.1002/jmri.24488
33. Marik W, Nemec SF, Zbýň Štefan, Zalaudek M, Ludvik B, Riegler G, et al. Changes in cartilage and tendon composition of patients with type I diabetes mellitus: identification by quantitative sodium magnetic resonance imaging at 7 T. *Invest Radiol* 2016; **51**: 266–72. doi: https://doi.org/10.1097/RLI.0000000000000236